SIMULATING CONVOLUTED MODERATORS

F. X. Gallmeier, E. B. Iverson, W. Lu, ORNL, Oak Ridge U.S.A.
G. Muhrer, LANL, Los Alamos, U.S.A.
D. V. Baxter, Indiana University, U.S.A.
E. Klinkby, ESS, Lund, Sweden

Abstract

It is a continuous effort at spallation sources to improve and optimize the directional emission of thermal and sub-thermal neutrons off the moderator faces into beam tubes. Tools have been upgraded to be able to simulate the emission improvements of so-called convoluted moderators, heterogeneous moderators of layered moderator and single crystal plates. The MCNPX code was equipped with a single-crystal neutron scattering model, and neutron reflection/refraction physics. Studies of simple cylindrical convoluted moderator systems of 100 mm diameter and composed of polyethylene and single crystal silicon were performed with the upgraded MCNPX code and reproduced the magnitude of effects seen in experiments compared to homogeneous moderator systems. Applying different material properties for refraction and reflection, and by voiding silicon, we could show that the emission enhancements are primarily caused by the transparency of the silicon/void layers. Parameter studies of the thicknesses of the polyethylene and silicon layers were conducted and arrived at optimal thicknesses of 1.3 mm for polyethylene and 1 mm for silicon.

INTRODUCTION

On the quest of improving the neutron emission from neutron moderators, which could benefit beam driven applications at neutron sources, a laboratory driven research project at the Oak Ridge National Laboratory investigated the neutron performance of moderating media interleaved with single-crystal layers or void layers (convoluted moderators). The experiments conducted at the LENS facility of Indiana University showed enhancements of neutron emission of about 40% in the thermal range at an angle 0.8 degrees off the plane using 2-mm-thick polyethylene layers and 0.7-mm-thick single-crystal silicon layers compared against the same size bulk polyethylene moderator.[1] Slightly higher enhancements were obtained by replacing the silicon by air (realized by spacers).

Experiments of testing prototypic moderator setups are tedious and allow only a very restricted parameter space to be tested. Therefore an effort was launched to develop and qualify tools for simulating heterogeneous moderator systems to enable target station design analysis for neutron sources involving such complex structure.

Convoluted moderators exploit the transparency of low-mosaic single crystals such as silicon and maximize the impact of its transparency by extracting neutrons at small angles with regard to the planes of the layered structures. All general purpose transport codes (MCNP{X}, GEANT4, PHITS, FLUKA) lack transport capabilities in single crystals and are not capable of simulating the transparency of these materials nor Bragg scattering effects. Furthermore refraction/reflection effects of neutrons at material interfaces based on differences of coherent scattering lengths of the materials are completely neglected. Both of these shortcomings are being addressed implementing extensions to MCNPX, the workhorse for characterizing target station and moderator neutron performance at SNS [2].

The upgraded MCNPX code [3] was then applied to demonstrate the new capabilities on simple convoluted moderator models.

SINGLE CRYSTAL TRANSPORT

Convoluted moderators seek to make use of the transparent property of single crystals unless any Bragg condition is satisfied. In addition Bragg scattering may be exploited to enhance the leakage of neutrons of selected energy from moderators into beamlines. Transparent solid media are especially needed in combination of liquid moderator materials where layer-type void spaces are otherwise impossible to engineer.

The multi-particle transport code MCNPX defines CAD-type geometry models from a multitude of cells being defined by Boolean algebra of from surfaces. Each cell is associated to a material. A material is composed of a mix of isotopes described by a M-card, for which the transport and scattering is described either by nuclear cross sections or by event generators. In the thermal and subthermal energy-range the influence of structural and dynamical material properties on the neutron transport are considered by utilizing thermal scattering kernels assigning kernel IDs to isotopes of a material composition through the MT-card. The scattering kernels describe coherent and incoherent elastic and inelastic scattering events on materials without long-range order (poly-crystals, liquids). This formalism is not adequate for describing single crystals, because it lacks the ability of having material orientation and scattering cross sections dependent of the incoming and outgoing neutron directions.

Two extensions were programmed into MCNPX:

- An association of the orientation of crystal axes with regard to the three directions of the global coordinate system on the cell basis;
- Implementation of a single crystal material properties and a single crystal scattering model.

As single crystal scattering depends on the relative angle between the incident neutron wave vector and the crystal planes, the orientation is an important crystal property and entered as a transformation matrix to each cell with single-crystal material specification through the newly defined MCNPX input card OCTR. In this way, single crystal assignments of the same material definition but with different orientation can be used in a problem definition, i.e. for setups of a facetted focusing monochromator or orientation variances of the many single crystal wafers of a convoluted moderator. During particle tracking, the neutron flight direction is transformed into the single-crystal coordinate system upon entering the crystal and transformed back into the local MCNPX coordinate system upon leaving the crystal. This formalism avoids having to provide single-crystal datasets for every different crystal orientation.

For performing single crystal scattering, the single crystal model from the McStas neutron optics package [4] was implemented, which describes neutron scattering of mosaic crystals and builds on information of lattice constants and a list of reciprocal lattice vectors including the structure factors for which Bragg scattering is allowed. A newly defined MC-card was implemented to flag the existence of single crystal scattering for a specific material definition, and to provide the filename of a single-crystal data file, the lattice spacing variance, and crystal mosaicity. The single crystal data file contains information of the crystal's unit cell vectors, the crystallographic planes and their structure factors. The existence of a MC-card overrides the material's elastic scattering information that may have been provided by the scattering kernel formalism through the MT card but still utilizes the inelastic scattering information from the scattering kernel. In this regard, a single crystal card is a refinement of neutron material interactions. The nuclear absorption is still governed by the evaluated nuclear data formalism disregarding any abnormal absorption effects that may be associated with single crystals. Incoherent elastic scattering due to isotope distributions is so far neglected.

Test runs were performed for comparing results of McStas with its original single crystal model and MCNPX and its newly implemented model. Fig. 1 shows the scattering map of a mono-directional neutron ray with about 11 meV energy incident on the crystal oriented with the crystal plane with Miller indices of (4 0 0) at perfect Bragg backscattering condition. The backscattering signal at theta of 180 degrees competes with reflections of the (2 2 0) plane (spots at [theta,phi]=[90,90] in degrees). MCNPX exhibits identical scattering behaviour signalling a successful implementation of the single crystal model.

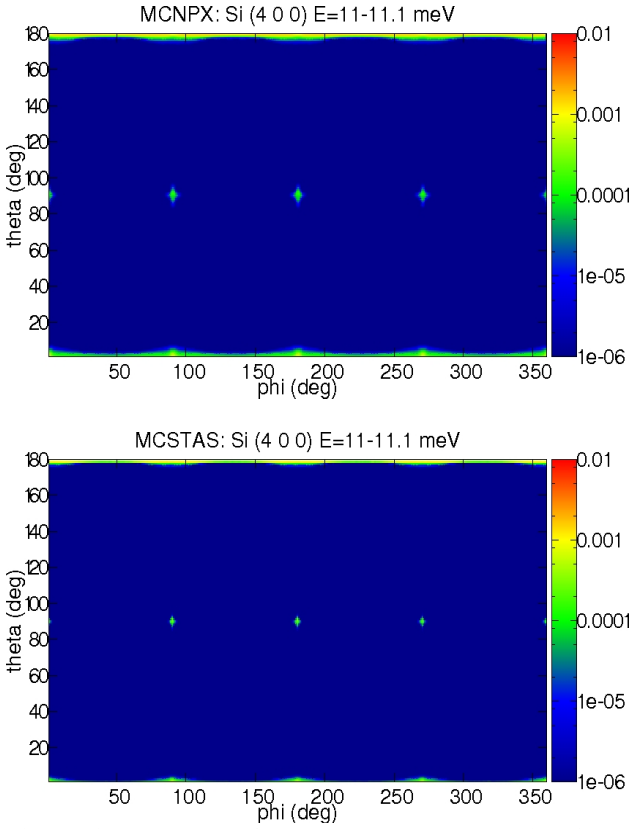

Figure 1: Neutron reflexes due to a mono-directional neutron beam incident on a 1-mm-cube single crystals oriented in (4 0 0) direction in perfect backscattering simulated with MCNPX (top) and McStas (bottom).

SILICON SCATTERING KERNEL

While coherent elastic scattering in silicon is treated by the single crystal model, for competing inelastic interactions the MCNPX code still relies on getting provided information through the scattering kernels of the respective material. Although scattering kernels are at best formulated for poly crystals, this was an approximation we accepted for now. In absence of scattering kernels for silicon, our prime candidate for a single crystal material, a kernel was developed for this material.

REFLECTION AND REFRACTION AT MATERIAL INTERFACES

Neutron refractive effects at material boundaries are typically neglected in general transport codes because of the low significance in general radiation transport problems. Neutrons do generally deviate from the straight flight path at material boundaries although these deviations tend to be small. These effects come into play for neutron transport mostly at sub-thermal energies, are responsible for neutron refraction and reflection at shallow incident angles, and are exploited for neutron mirror and guide systems.

Formalism

Refraction and reflection of neutrons at material boundaries are effects described by the Schrödinger equation having a neutron plane wave with wave vector ***k*** incident on a potential well as formulated by physics text books such as Neutron Optics by Sears [5]. The material specific potential V is determined by the sum of coherent scattering lengths of the material isotopes weighted by its number densities.

The potentials are of the order of 10^{-6}-10^{-5} eV for condensed matter, are typically positive, but can be negative for selected materials especially for hydrogenous materials due to the negativity of the hydrogen scattering length.

The difference of the material potentials $(V_1 - V_2)$ let us define a critical perpendicular wave vector k_c by

$$k_c^2 = \frac{2m_n}{\hbar^2}(V_1 - V_2) \qquad (1)$$

where the neutron penetrates the material interface from material 1 into material 2.

The continuity of the wave function requires only the component normal to the surface to experience a change due to the potential difference of the materials (here the indices 1 and 2 refer to the incident and final neutron beam) and the :

$$k_{2\perp} = \begin{cases} \sqrt{k_{1\perp}^2 + k_c^2}, & k_{1\perp}^2 > k_c^2 \\ -k_{1\perp}, & k_{1\perp}^2 < k_c^2 \end{cases} \qquad (2)$$

Continuity of the wave function and its derivative define the probability of transmission T, meaning the neutron passing by refraction from one material into the other, which can be derived to

$$T = \left(\frac{2\,k_{1\perp}}{k_{1\perp}+k_{2\perp}}\right)^2. \qquad (3)$$

At conditions close to the critical wave vector, reflection and refraction are competing effects governed by equation 3.

Implementation

Upon request of the refraction/reflection option (a flag entered as 8th entry in the PHYS:N card), the coherent neutron scattering lengths are read from a data file compiled from Sears [6] for all elements and isotopes, and the material potentials V are calculated automatically for all materials in the problem by a newly implemented subroutine. Reflection and refraction is performed at boundary crossing for neutrons below the energy of 100 eV according to the above described formalism involving changes of the flight direction and adjustments of the energy according to the materials' potential difference. Refraction angles inning up in the interface tangential plane and may cause problems in the particle tracking formalism are avoided by enforcing a lower bound of the cosine with regard to the surface normal of 10^{-6}. All this treatment is provided by a newly implemented subroutine being called at intersection of surfaces during particle tracking.

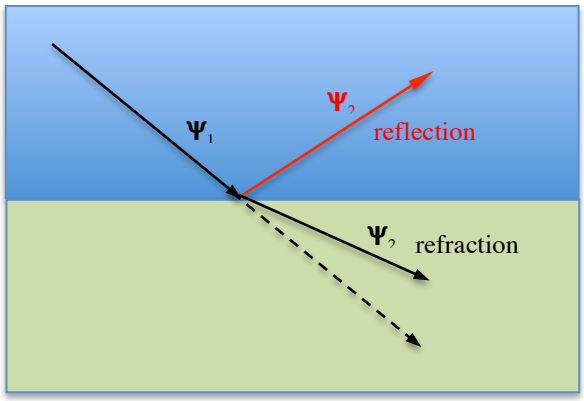

Figure 2: Neutron wave functions in refraction (black) and reflection (red).

The refraction/reflection capability causes some limitations: it reduces the functionality of point detector and pin-hole tallies to neutron energies above 100 eV. Point detectors count on straight flight-path extensions from the last collision point to the detector point, an assumption that is no longer valid when reflection and refraction physics is being applied. Furthermore, the possibility arises that very-low-energetic neutrons are being caught in a material trap through total reflection at the material interfaces and cause a non-terminating neutron trajectory an effect that is actually exploited by building neutron bottles for ultra-cold neutrons[7].

CONVOLUTED MODERATOR SIMULATIONS

First convoluted moderator setups were evaluated in simple cylinder-symmetric models of moderators of 100 mm diameter and height that are fed by a source neutrons of epithermal (1/E) energy distribution in the energy range of 10-10^5 eV starting at a spherical surface with 200 mm diameter with the moderator in its center as sketched in Fig. 3. The neutrons start inward directed with flat angular distributions within 25 degrees with regard to the inward directed surface normal. For all the studies presented here, we assume polyethylene and silicon layers of various thicknesses stacked along the cylinder axis to fill all the moderator volume. As reference cases we used moderators of bulk polyethylene.

Because we are interested in moderators to produce neutron beams, calculations were performed mimicking ambient temperature and cold moderators using polyethylene scattering kernels at room temperature and at 77K, respectively. Silicon kernels were for room temperature and 20K.

The neutron emission from the moderator is scored at the cylindrical surface of the moderator binned in energy by logarithmically spaced bins with 10 bins per decade, and binned in angle with regard to the cylinder axis in bins of 0.1 degree spacing between 87 and 93 degrees. This quasi two-dimensional setup allows to study so-called geometric and reflection/refraction effects, however, is because of integrating in the azimuthal angle fairly

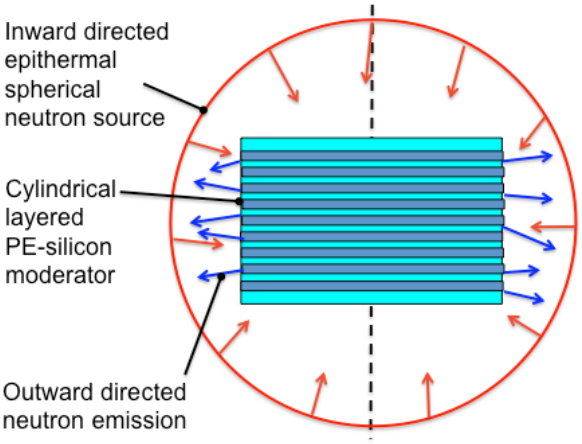

Figure 3: Layout of the two-dimensional model

insensitive to Bragg phenomena. The silicon crystal was oriented with the crystallographic plane described by the (1 1 1) Miller index aligned with the cylinder axis.

MCNPX runs of 10^9 neutrons took about 8000 CPU minutes per analyses and an aged computer cluster of 70 CPUs provides a reasonable fast 2-3 hours turn around of a calculation delivering results with relative statistical errors of one standard deviation of below 0.5% in the energy bins of the spectral peak. The simulations including Bragg scattering took twice the time. Resulting neutron emission distributions in angle and energy are shown in Fig. 4 for the bulk PE, and the case with 2.3-mm-thick PE and 0.7-mm-thick silicon.

Evidently, the layering causes the emission into a double-humped peak at 89.2 and 90.8 degrees with regard to the cylinder axis (or at about ± 0.8 degree with regard to the normal of the cylinder mantle surface). Voiding the silicon layers gives about 10% higher peak emission compared to the case with silicon layers. Fig. 4-bottom shows results with an artificially modified scattering length for hydrogen such that the potential difference of the materials sums up to the negative of the PE/silicon case. Again we obtain emission peaks at the same angles, but the central depression is more pronounced with a canyon-type fall-off and widening in the angle domain towards lower energies. In this case at incident angle-energy combinations falling within the valley neutron reflection prevents the neutrons from entering the silicon layers.

Parameter studies were conducted to assess the impact of the peak intensity and peak location varying the silicon thickness from 0 to 1mm at constant PE thickness of 2.3 mm PE, and varying the PE thickness from 0.7 to 3.1 mm at constant 0.7 mm silicon thickness at the PE temperature of 77 K. Angular emission distributions in the spectral peak at 9.33 meV are shown in Fig. 5. The peak heights increase with PE thickness from 0.7mm peaking at about 1.3 mm and fall slightly for increasing the thickness further. The angular peak location does not change with PE thickness.

The silicon thickness, however, strongly influences the angular peak location moving to larger angles for

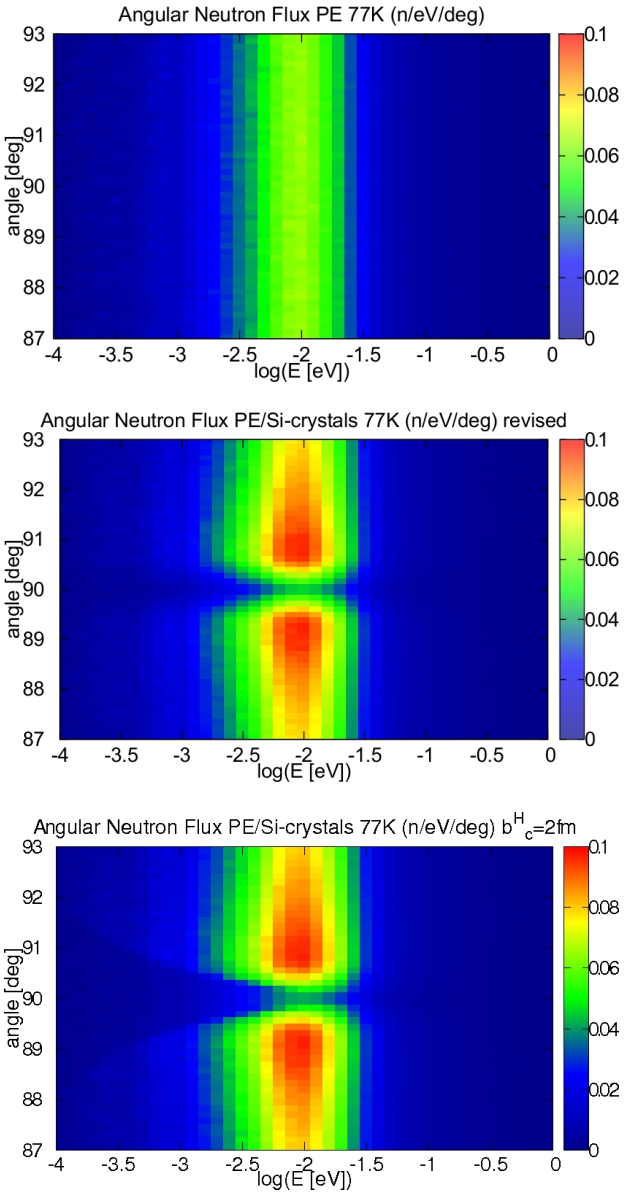

Figure 4: Maps of neutron emission in angle and energy from with regard to the cylinder axis: bulk polyethylene (top), 2.3 mm polyethylene 0.7 mm silicon layering (center), negative potential difference of polyethylene and silicon (bottom).

increased thickness at an increased peak height. At 1-mm silicon thickness the maximum was not reached, however, the changes beginning from 0.6 mm silicon thickness were marginal. Correlated with the peak height is the magnitude of central depression between the peaks. For the layer thickness combinations investigated here, we find an overall gain in neutron emission integrated over the angles between ±3 degrees; the increase of neutron emission by the silicon layers is more pronounced than the loss of moderator volume. For the 300K moderators we saw qualitatively the same behaviour, the shoulder heights are reduced from about 55% for the 77K moderator to 45% very likely due to an increased inelastic scattering cross section at 300K in silicon.

CONCLUSION

Reflection/refraction physics and a neutron single-crystal scattering model were implemented into MCNPX for investigating phenomena of convoluted (layered) moderator structures that have exhibited improvements of neutron emission at off-normal directions with regard to the emission surface in experiments. In simple models, the enhancements were duplicated in simulations of layers of PE and silicon applying the modified MCNPX code. The magnitude of the enhancements and also the angular peak locations agree with the experimental findings. The enhancements are mainly attributed to the transparency of the silicon layers as void layers proved to demonstrate the same effects; refraction/reflection effects play a secondary order role. The peak heights of neutron emission depend mainly on the thickness of the polyethylene layer peaking at 1.3 mm thickness, whereas the location of the peaks is influenced by the silicon thickness moving to larger off-center angles for increased thickness.

REFERENCES

[1] Iverson E. B. et al, Enhancing Neutron Beam Production with a Convoluted Moderator, NIMA, to be published 2013.

[2] Lu W. et al, Improved moderator performance calculations at SNS, Tenth International Topical Meeting on Nuclear Applications of Accelerators (AccApp'11), April 3-7, 2011, Knoxville, Tennessee, USA.

[3] Pelowitz, D. B., MCNPX User's Manual, Version 2.6.0, Report LA-CP-07-1473, Los Alamos National Laboratory, Los Alamos, New Mexico, USA, 2008.

[4] Willendrup, P., et al. User and Programmers Guide to the Neutron Ray-Tracing Package McStas, Version 1.12, Materials Research Department, Risø DTU, Roskilde, Denmark (2008).

[5] Sears V. F., Neutron Optics, Oxford University Press, New York, 1989.

[6] Sears V. F., Neutron scattering lengths and cross sections, Neutron News, Vol. 3, 1992

[7] Goeltl, L., The Ultra-cold Neutron Source at PSI, Tenth International Topical Meeting on Nuclear Applications of Accelerators (AccApp'11), April 3-7, 2011, Knoxville, Tennessee, USA.

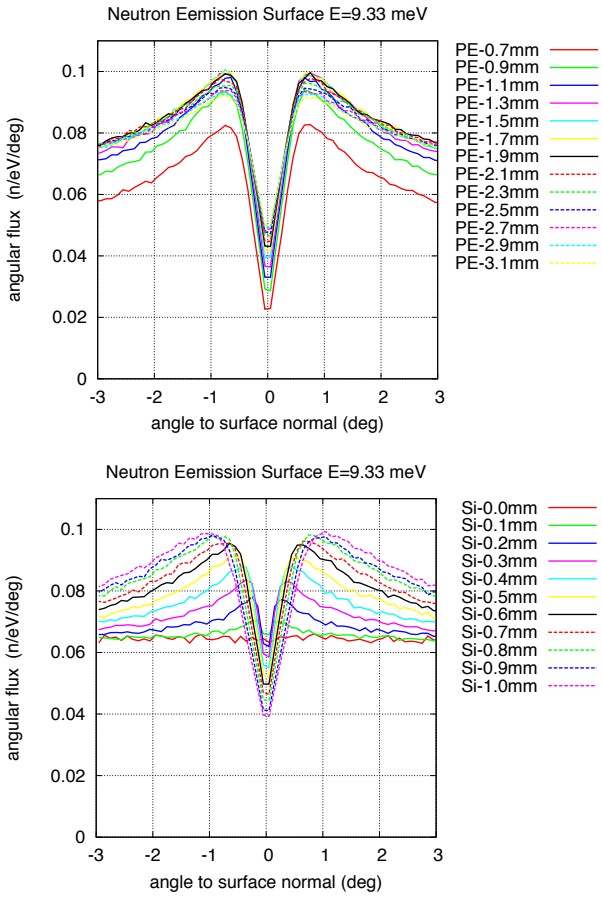

Figure 5: Variation of PE thickness at silicon thickness of 0.7 mm (right), and variation of silicon thickness at PE thickness of 2.3 mm for 77K temperature.